



**ADDITIONAL MATERIALS AVAILABLE ON THE
HEI WEBSITE**

Research Report 212

**Mortality–Air Pollution Associations in Low Exposure Environments
(MAPLE): Phase 2**

Michael Brauer et al.

**Additional Materials A. Collection of Measurements at
MAPLE/SPARTAN Sites**

**Additional Materials B. Sensitivity of Estimates of Excess Deaths
Attributable to PM_{2.5} Exposure in Canada Due to Form of Relative Risk
Model and Characterization of Low Concentration Uncertainty**

These Additional Materials were not formatted or edited by HEI. This document was part of the HEI Low-Exposure Epidemiology Studies Review Panel's review process.

Correspondence may be addressed to Dr. Michael Brauer, The University of British Columbia, School of Population and Public Health, 366A – 2206 East Mall, Vancouver, BC V6T1Z3, Canada;
e-mail: michael.brauer@ubc.ca.

Although this document was produced with partial funding by the United States Environmental Protection Agency under Assistance Award CR–83467701 to the Health Effects Institute, it has not been subjected to the Agency's peer and administrative review and therefore may not necessarily reflect the views of the Agency, and no official endorsement by it should be inferred. The contents of this document also have not been reviewed by private party institutions, including those that support the Health Effects Institute; therefore, it may not reflect the views or policies of these parties, and no endorsement by them should be inferred.

© 2022 Health Effects Institute, 75 Federal Street, Suite 1400, Boston, MA 02110

HEI Research Report 212 Brauer Additional Materials – Available on the HEI Website

Additional Materials A. Collection of Measurements at MAPLE/SPARTAN Sites

We expanded the Surface PARTiculate mAtter Network (SPARTAN) (Snider et al. 2015) to routinely collect colocated measurements of $PM_{2.5}$, aerosol scatter, and AOD at five sites across Canada. This collection allows us to evaluate and potentially improve simulations of the $PM_{2.5}$ to AOD ratio in regions of low $PM_{2.5}$ mass concentrations. A key source of uncertainty in this relationship is the mass scattering efficiency (MSE), the relation between particle scatter and $PM_{2.5}$ mass. Mass scattering efficiency is fundamental to the measurement of AOD and influences the accuracy of $PM_{2.5}$ estimates as GEOS-Chem simulates the columnar AOD to surface $PM_{2.5}$ relationship. The mass scattering efficiency generally varies smoothly across large distances (Latimer and Martin 2019). Thus, only a moderate number of measurement locations across Canada are needed to evaluate the simulated MSE. As no routinely collected measurements of MSE were available in populated regions of Canada, these targeted ground-based measurements offer the potential to evaluate and improve these estimates.

Measurements include an impaction filter sampler for analysis of mass and composition, as well as a nephelometer that provides high temporal resolution to relate observations during cloud-free conditions at satellite overpass time to 24-hour averages. The combination of scatter and mass measurements allow for an assessment of the relationship between satellite measurements of backscattered sunlight and the $PM_{2.5}$ mass concentrations. These measurements are compared with GEOS-Chem simulations of the AOD to $PM_{2.5}$ relationship to better understand the geophysical processes affecting the relationship, and in turn to improve the ability of chemical transport models to predict this quantity.

Specifically, we added $PM_{2.5}$ monitors to five ongoing and diverse Canadian sites participating in the global Aerosol Robotic Network (AERONET, <http://aeronet.gsfc.nasa.gov/>) that routinely measure AOD. Figure A.1 shows the locations of the colocated $PM_{2.5}$ and AOD measurement sites in Halifax, Nova Scotia; Sherbrooke, Quebec; Downsview, Ontario; Lethbridge, Alberta; and Kelowna, British Columbia.

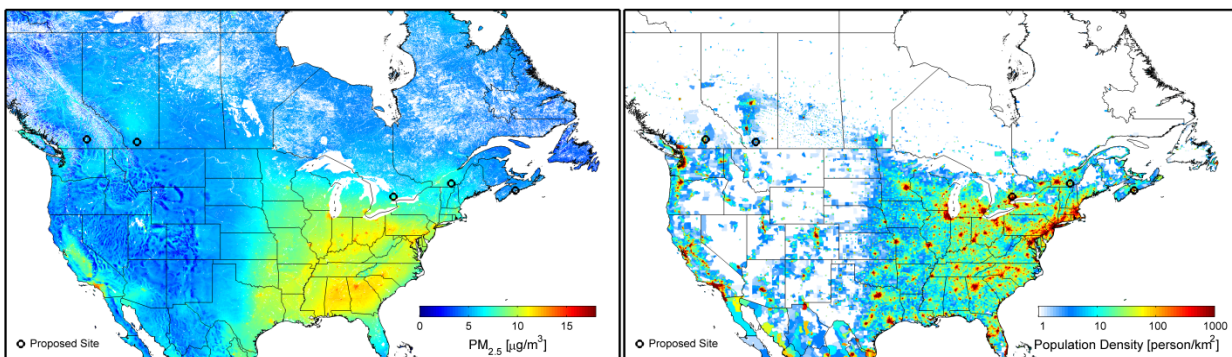


Figure A.1. Location of collocated ground-based measurements of PM_{2.5} and AOD. The background shows satellite-based estimates of PM_{2.5} from van Donkelaar et al. (2016) (left), and population density (right).

Sampling instrumentation included an AirPhoton SS5 Series impaction filter sampler and AirPhoton 3-wavelength integrating nephelometer. The combination of integrated filter samples with high temporal resolution scatter measurements offer the ability to infer characteristics of PM_{2.5} on 24-hour time scales and relate optical observations at satellite overpass time to 24-hour mass averages.

Particulate matter (PM_{2.5} and PM₁₀) was collected on pre-weighed PTFE filters loaded into a protective 8-slot cartridge that includes one travelling blank, six sequentially active PM_{2.5} filters, and one regularly active PM₁₀ filter that samples intermittently throughout each 9-day PM_{2.5} sampling period. The PM_{2.5} filters sample 48 hours over one diurnal cycle in the 9-day period ending at 09:00 local time. The sampling period is designed to end when temperatures are low to reduce the loss of semi-volatile chemical components. When sampling is complete the cartridges were shipped in sealed containers under ambient conditions to the Dalhousie University laboratory for chemical analysis. A detailed explanation of SPARTAN chemical analysis methodology and filter-based hygroscopicity parameter, κ , are provided by Snider et al. (2016). Briefly, all gravimetric analysis was performed in a cleanroom facility with controlled temperature between 20 to 23 °C and a relative humidity at $35 \pm 5 \%$, following U.S. EPA protocols. Flow rates at ambient pressure and temperature at site locations determine the sampled air volume to provide PM_{2.5} concentrations in $\mu\text{g}/\text{m}^3$. Black carbon (BC) content was estimated from triplicate measurements of surface reflectance using a smoke stain reflectometer. Filters were subsequently analyzed for water-soluble ions (e.g. sulfate, nitrate, ammonium) through ion chromatography and trace elements, including dust components (e.g. aluminum, iron, magnesium), via inductively couple plasma-mass spectrometry and x-ray fluorescence

spectrometry. Trace element measurements are described in McNeille et al. (2020). As described in Snider et al. (2016), the residual matter (RM) component, estimated by subtracting the dry inorganic mass and particle-bound water from total $PM_{2.5}$ mass, is treated as predominately organic.

The nephelometer operates entirely autonomously, recording ambient total scattering and backscattering data at three wavelengths (457, 532, 634 nm), at a frequency of once every 15 seconds. Measured scatter is converted to 550 nm via a fitted Ångström exponent. Hourly scatter values for which relative humidity (RH) is greater than 80% are excluded to reduce uncertainty in accounting for aerosol water (Snider et al. 2016). Hourly scatter above $2500 Mm^{-1}$ were also screened as high aerosol concentrations saturate the nephelometer leading to a nonlinear response. To account for transient meteorological events a derivative-based screening protocol, similar to the approach used by the IMPROVE network, was applied to screen hourly scatter values where the change is greater than $\pm 50 Mm^{-1} hour^{-1}$. Relative fluctuations in total scatter (b_{sp}) are anchored to an absolute filter mass to infer hourly average $PM_{2.5}$ concentrations following the equation:

$$PM_{2.5, hourly} = [PM_{2.5, 9-day}] \frac{b_{sp, hour}}{b_{sp, 9-day}}$$

Daily $PM_{2.5}$ estimates are then calculated by taking the mean of available hourly values.

Ground based aerosol optical depth at satellite overpass time ($AOD_{overpass}$) is defined as the measurement of AOD reported by AERONET (Holben et al. 1998) averaged from 10:00 to 12:00 and 13:00 to 15:00 local time to include a range of satellite overpass times. AERONET provides multi-wavelength AOD measurements with a low uncertainty of < 0.02 (Holben et al. 2001). All-points level 2.0 or 1.5 cloud screened data are used at all sampling sites. The AOD is interpolated to 550 nm via the Ångström exponent.

The Downsview MAPLE site was collocated with a NAPS site run by Environment and Climate Change Canada that included two sampling stations that are compared with MAPLE measurements. The first, a Dichotomous Manual Air Sampler (2000i-D Partisol Thermo) that samples $PM_{2.5}$ mass on a Teflon filter, is considered the NAPS reference method. The second sampler is a Met One SuperSASS-Plus Sequential Speciation Sampler (SASS). Both samplers follow the same schedule and collect every 1-in-3 days from 00:00 to 24:00 local standard time. Daily $PM_{2.5}$ mass concentrations from MAPLE are estimated using a combination of filter sample data and time-resolved nephelometer measurements as described above. A minimum of 12 hourly points are required to create a 24-hour mean value.

Comparison of daily PM_{2.5} mass concentration is completed using estimated daily PM_{2.5} from MAPLE versus the NAPS reference method sampler (Partisol). For speciation comparison, NAPS data from the SASS sampler are sampled coincidentally with the MAPLE integrated filter sample; if a MAPLE filter sampled August 8–16, 2018, any daily NAPS filter sample(s) from the corresponding time period (e.g., August 9, 12, and 15 2018) are used to create a mean value.

Additional Materials B. Sensitivity of Estimates of Excess Deaths Attributable to PM_{2.5} Exposure in Canada Due to Form of Relative Risk Model and Characterization of Low Concentration Uncertainty

We have shown a positive association between nonaccidental mortality and long-term exposure to PM_{2.5} throughout the observed concentration range from 2.5 µg/m³ to 17.7 µg/m³. The lower uncertainty bound is greater than unity above 2.9 µg/m³ indicating a high degree of confidence that reductions in exposure will result in reductions in the mortality rate and thus increases in life expectancy. We have, however, no evidence from this study that reductions below the lowest observed concentration of 2.5 µg/m³ will translate into a decrease in mortality risk. In addition to the *eSCHIF* concentration–mortality characterization, we fit a standard threshold model, *THRES*, whose lower uncertainty bound was greater than unity for concentrations above 3.5 µg/m³.

There have been other characterizations of the shape of the PM_{2.5}–mortality association and its uncertainty at low concentrations. Most notably is that of the Global Burden of Disease (*GBD*) program (GBD, 2020). *GBD* estimates of attributable mortality and burden of disease are based on a contrast between current exposure and a less-polluted counterfactual (*cf*) exposure. *GBD* identifies the minimum exposure soliciting a positive risk, termed Theoretical Minimum Risk Exposure Level (*TMREL*). Below the *TMREL* no change in risk is assumed to exist (GBD, 2020). *GBD* assumes there is a range in concentration for the *TMREL*, thus assuming an uncertainty distribution. The range is 2.4 µg/m³ to 5.9 µg/m³, and is calculated as the average of the minimum and 5th percentiles of concentrations for cohorts whose 5th percentile is below that of the American Cancer Society Cancer Prevention II cohort (Turner et al., 2015) of 8.2 µg/m³. *GBD* stochastically characterizes the *TMREL* as a uniform distribution with lower and upper bounds of 2.4 µg/m³ and 5.9 µg/m³ respectively.

We apply the *TMREL* to the *Log – Linear* model, *LL*, as: $LL(z) = \exp(\beta_{LL}(z - TMREL))$ if $z \geq TMREL$ and unity otherwise. For any concentration z , we calculate 1,000 predictions by first simulating 1,000 realizations from $TMREL \sim U(2.4, 5.9)$ and 1,000 realizations of $\beta_{LL} \sim N(\hat{\beta}_{LL}, \hat{\sigma}_{\hat{\beta}_{LL}})$ where $\hat{\beta}_{LL}$ is the estimate of β_{LL} and $\hat{\sigma}_{\hat{\beta}_{LL}}$ its estimated standard error. We consider the example of nonaccidental mortality with $\hat{\beta}_{LL} = 0.0081$ and $\hat{\sigma}_{\hat{\beta}_{LL}} = 0.0005$.

We obtained the number of deaths for the population over the age of 25 years and PM_{2.5} for all 293 census divisions (*CD*) in Canada, averaged over the three-year period 2015-2017 (Health Canada, 2021). We calculate the attributable fraction, *AF*, defined by:

$$AF(z_i) = 1 - \frac{1}{RR(z_i)}$$

where z_i , is the PM_{2.5} concentration in the i^{th} census division.

Estimates of excess annual deaths are calculated by multiplying the number of deaths in each census division by its corresponding attributable fraction and summed over census divisions. We assume that mortality counts are known without error but the relative risk is characterized with uncertainty. This calculation is repeated 1,000 times using parameter estimates drawn from their respective uncertainty distributions for the three models: *eSCHIF*, *THRES*, and *LL*. The central estimate is given by the mean of model predictions with 95% confidence intervals defined by the 2.5 and 97.5 percentiles of the uncertainty distribution.

The mean relative risk predictions and 95% confidence intervals are displayed in Figure B.1 by model form (Panel A) over the Canadian PM_{2.5} range (0.6µg/m³, 8.8µg/m³). The *eSCHIF* mean predictions tend to be greater than the *THRES* predictions over much of the concentration range with the *LL* model incorporating the *TMREL* counterfactual less still. The *eSCHIF* has a pronounced supra-linear shape while the *THRES* has a slight sub-linear shape, with the *LL* model predictions displaying a more pronounced sub-linear shape. The 95% confidence intervals of the *eSCHIF* do not overlap those of either the *THRES* or *LL* models except for the very lowest concentrations. However, the *THRES* and *LL* confidence intervals do overlap.

The Canadian population PM_{2.5} distribution is presented in Panel B with the *TMREL* concentration range (yellow x-axis tick marks). Population-weighted mean concentration is 6.14µg/m³ with 1% of Canadians living in census divisions below the *TMREL* lower limit of 2.5µg/m³ and 44% living below the upper limit of 5.9µg/m³.

The relative risk comparisons are reflected in the estimated uncertainty distributions of the number of annual attributable deaths estimates based on 100% reduction in PM_{2.5} concentrations (Panel C). The *eSCHIF* based mean estimate (14,172 deaths) is more than twice that of the *THRES* based estimate (6,927 deaths) and more than three times that of the *LL* model incorporating the *TMREL* counterfactual (4,208 deaths). The *eSCHIF* uncertainty distribution is greater than and does not overlap either the *THRES* or *LL* uncertainty distribution (Figure B.1, Panel C).

Our analysis suggests that health burden estimates can be sensitive to both the shape and uncertainty characterization of the relative risk function.

REFERENCES

GBD 2019 Risk Factor Collaborators, 2020. Global burden of 87 risk factors in 204 countries and territories, 1990–2019: a systematic analysis for the Global Burden of Disease Study 2019. *Lancet* 396, 1223-1249, doi:[https://doi.org/10.1016/S0140-6736\(20\)30752-2](https://doi.org/10.1016/S0140-6736(20)30752-2).

Health Canada (2021). <https://www.canada.ca/en/health-canada/services/publications/healthy-living/2021-health-effects-indoor-air-pollution.html#a3.2>

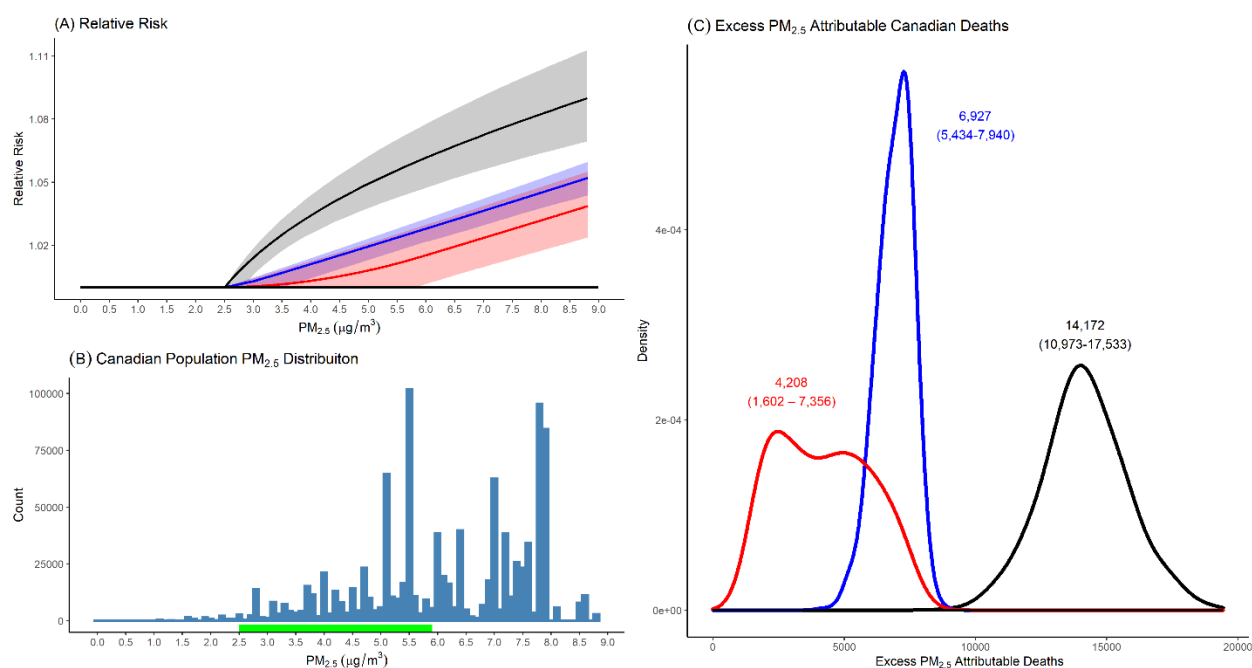


Figure B.1. *eSCHIF* (mean - black line; uncertainty interval – grey shaded area), *THRES* (mean - blue line; uncertainty interval – blue shaded area), and *Log – Linear* with *TMREL* counterfactual (mean – red line; uncertainty interval – pink shaded area) predictions over Canadian concentration range (Panel A). Canadian population PM_{2.5} distribution (Panel B) with *TMREL* concentration range (x-axis yellow tick marks). Uncertainty distribution of number of excess deaths attributable to PM_{2.5} exposure in Canada based on *eSCHIF* (black line), *THRES* (blue line), and *LL* with *TMREL* counterfactual (red line) (Panel C). Annotations depict mean number of excess deaths with 95% confidence interval in parentheses.